

# Non-hierarchical UAV Formation Control for Surveillance Tasks

Dirk van der Walle, Barış Fidan, Andrew Sutton, Changbin Yu and Brian D.O. Anderson

**Abstract**—In this paper, we consider motion and formation control of a team of three unmanned aerial vehicles (UAVs) for a particular surveillance task. The UAVs are required to fly in an equilateral triangle formation (to optimize target location estimation accuracy), with the centre of mass following a nominated (spiral) trajectory, which reflects the constraints on the turning radius of the flight paths. Furthermore, the UAVs need to fly at constant and nearly (but not necessarily exactly) the same speeds. A decentralized control scheme is designed and analyzed for the above motion and formation control tasks, based on a non-hierarchical (i.e. three-coleader) sensing/control structure.

## I. INTRODUCTION

In recent years, multi-agent mobile robotic systems have started being used in various fields to perform a variety of tasks [1]–[3]. The mobile robotic agents used in these applications include ground, air, marine, underwater vehicles or robots. A particular class of tasks for such multi-agent robotic systems involve surveillance of a region and tracking of targets cooperatively [2], [4], [5]. The main reasons for performing such tasks cooperatively may be quite different for different cases, and range from insufficiency of a single agent for performing a particular task (e.g. localization using bearing-only-measurements) to requirements of robustness against agent losses or optimality in terms of accomplishing the tasks faster and more accurately. Again because of various requirements such as having a fixed well-defined control/sensing/communication architecture or maintaining optimal geometries of the agents relative to each other for the particular mission of interest, the multi-agent robotic system may be required to maintain a formation while performing a surveillance or target localization/tracking task [4], [5].

In this paper, we consider cooperative surveillance over a 2-dimensional region of interest using a team of three unmanned aerial vehicles (UAVs). The particular surveillance task we focus on, whose further specifications are given in Section II, is part of a research challenge problem posed by the Australian Defence Science and Technology Organisation (DSTO) on localization of targets with mobile sensors over large areas of interest. In this task, the three UAVs are equipped with bearing-only (or angle-of-arrival)

measurement sensor units and are required to localize signal emitting targets using the bearing measurements they obtain while surveying cooperatively.

To obtain reliable results in such a bearing-only-measurement-based localization task, cooperation of at least three agents, as in our case, is necessary; and furthermore, the formation geometry of the 3-UAV team is important for accuracy of the localization results [4], [6], [7]. In our case, it is desired that the 3-UAV team maintains an equilateral triangular formation (which is the optimal geometry for bearing-only-measurement-based localization with three agents [4], [6], [7]) while the center of mass (CM) of the formation is tracking a predefined spiral shaped path in the region of interest. In order to maintain the desired formation during surveillance, the distance between each of the three pairs of agents within the formation needs to be kept as close as possible to a certain pre-defined constant value.

In Section III, we develop a *non-hierarchical* formation control scheme for the particular cooperative surveillance described above. Here, we use the term *hierarchy* in terms of distribution of various control tasks such path tracking and inter-agent distance keeping. By being *non-hierarchical*, we require the subtasks of decentralized control scheme to be uniformly distributed among agents.

A particular constraint in the above cooperative control task is that the UAV agents used in the control task (the *Aerosonde* UAVs [8] in the actual real-time implementation) fly at constant and nearly (but not necessarily exactly) the same speeds. Here, flying at constant speeds constrains the UAV agent dynamics while the possible difference between the constant speeds appears to be a phenomenon that significantly affects the formation maintenance task during motion. Hence two particular challenges are designing the individual agent control laws to comply with constant agent speeds, and guaranteeing formation maintenance robustly to disturbances and uncertainties caused by the difference between constant agent speeds.

The non-hierarchical control scheme developed in Section III is analyzed via a series of numerical simulations in Section IV in order to demonstrate its performance characteristics and robustness to inter-agent speed differences and external (wind) disturbances. The paper is concluded with some final remarks in Section V.

## II. SURVEILLANCE ON A SPIRAL PATH

In this section we give detailed specifications of the cooperative surveillance task introduced in Section I and the 3-UAV formation to be used for this task.

D. van der Walle is with Delft Center for Systems and Control, Delft University of Technology, Delft, the Netherlands [D.vanderWalle@student.tudelft.nl](mailto:D.vanderWalle@student.tudelft.nl)

B. Fidan, A. Sutton, C. Yu, and B.D.O. Anderson are with NICTA—National ICT Australia and the Australian National University, Canberra, ACT 2601, Australia {Baris.Fidan, u2548624, Brad.Yu, Brian.Anderson}@anu.edu.au

NICTA is funded by the Australian Government as represented by the Department of Broadband, Communications and the Digital Economy and the Australian Research Council through the ICT Centre of Excellence program.

## A. System Specification

The particular UAVs used for the surveillance task introduced in Section I are equipped with passive direction finding sensors and communication payloads. One particular motivation for the research is accurate cooperative localization of ground-based radar systems with a small-size UAV fleet [7]. This particular surveillance task is planned to be experimented by DSTO using UAVs of the type *Aerosonde* [8], a small UAV developed by Aerosonde Pty Ltd. An *Aerosonde* UAV typically has a wing span of 2.9 m and a maximum take-off mass of 15 kg. It can stay flying for 8–30 hours, depending on the payload it carries, without refueling.

The airspeed of the UAV is set to a constant value, between 20 m/s and 32 m/s, after take-off. Complying with the fixed constant (maximal) airspeed of 32 m/s and minimum turning radius of 400 m, the maximum turning rate is specified to be 0.08 rad/s.

The region of interest for surveillance is assumed to be a square with 30 km side length, and denoted by  $R_S$ , with its CM at the origin of the  $xy$ -coordinate system. For accuracy of localization of targets it is required to keep the inter-agent separation distances sufficiently large, nominally 3km, and for coordination and optimal/accurate geolocation purposes a constant equilateral triangle formation is required.

## B. UAV Agent Model

Each of the three UAVs is assumed to fly at a constant altitude ( $z$ -coordinate), parallel to the 2-dimensional region to be surveyed. Therefore we assume the region of surveillance to be over an  $xy$ -plane (where the  $z$ -coordinate is constant), and consider only the lateral ( $xy$ -coordinate) components of the UAVs' motion, positions, velocities, etc. Base on these assumptions, and labeling the individual agents as  $A_1$ ,  $A_2$  and  $A_3$ , each agent  $A_i$ ,  $i \in \{1, 2, 3\}$  is assumed to move with the kinematics

$$\begin{aligned} \dot{x}_i(t) &= v_{ci} \cos \theta_i(t) \\ \dot{y}_i(t) &= v_{ci} \sin \theta_i(t) \\ \dot{\theta}_i(t) &= \omega_i(t) \end{aligned} \quad (1)$$

where  $p_i(t) = (x_i(t), y_i(t)) \in \mathbb{R}^2$  ( $xy$ -plane),  $\theta_i(t)$  and  $\omega_i(t)$  are respectively the position, heading and angular velocity of each agent at time instant  $t \geq 0$ .

Each agent  $A_i$  is assumed to sense the location  $p_i(t)$  of itself as well as the position of the agent it has to follow, for all  $t$ . Furthermore each  $A_i$  is assumed to know the spiral path to be tracked by the formation's CM and hence the waypoints  $w_n$  defining this path, generation of which is explained in detail in Section II-D.

*Remark 1:* All the specifications given in Section II-A are practical ones supplied by the DSTO. Furthermore, the UAV agent kinematics model (1) is a practical model complying with the built-in aerodynamic controllers in the *Aerosonde* UAVs that convert given heading or waypoint commands to the actual control signals governing the motion of these UAVs.

## C. Cooperative Surveillance Task

The cooperative surveillance path tracking task using the 3-UAV formation, which is described in parts in the previous sections, is depicted in Figure 1. The particular surveillance path to be tracked is taken as an Archimedean spiral originating from a point close to the center of the region of interest,  $R_S$  (i.e. the origin of the  $xy$ -coordinate system). This spiral surveillance path can be formulated in time-indexed form in 2-dimensional polar coordinates  $(r, \bar{\theta})$  corresponding to the cartesian coordinates  $(x, y) = (r \cos \bar{\theta}, r \sin \bar{\theta})$ , with the starting point at  $(a, 0)$  (in both polar and cartesian coordinates), as

$$\begin{aligned} r(t) &= a + b\bar{\vartheta}(t) \\ \bar{\theta}(t) &= \bar{\vartheta}(t) \pmod{2\pi} \end{aligned} \quad (2)$$

where  $\bar{\vartheta}(t)$  is a monotonically increasing function of  $t$  satisfying  $\bar{\vartheta}(0) = 0$  and  $\lim_{t \rightarrow \infty} \bar{\vartheta}(t) = \infty$ , and the design constants  $a, b \geq 0$  denote, respectively, the initial radial offset and the radial increase rate of the spiral.

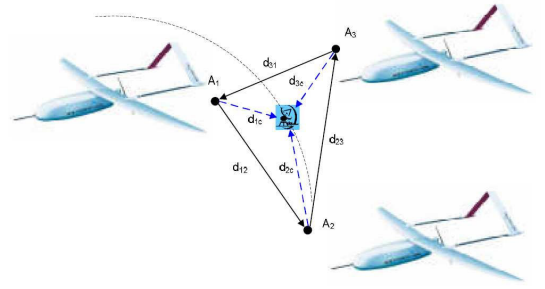


Fig. 1. Structure of a three-coleader formation. Each arrow in the graph depicts a distance maintenance constraint between two agents or between an agent and a target point on the spiral path.

Note that the results presented in this paper for this particular curve can be easily adapted to other smooth curves satisfying certain curvature constraints as well. Nevertheless there are certain practical motivations for using the spiral path (2). The spiral path (2) originating from  $(a, 0)$  scans the vicinity of the CM of  $R_S$ ,  $(0, 0)$  in a well-formulated polar form with constant increase rates of both the angle and radius. Hence tracking (2) would result in a smooth motion originating from the center of  $R_S$  and going towards the borders of  $R_S$ . Furthermore, an agent, actual or fictitious, following this path will have a continuously increasing turning radius and hence continuously decreasing turning rate. In (2), the periodicity rate of the scan angle  $\bar{\theta}(t)$  (modulo  $2\pi$ ) and the increase rate of the scan radius  $r(t)$  can be adjusted by selecting the spiral path parameters  $a, b$  accordingly.

Given the formulation of the spiral path to be tracked, the cooperative surveillance task above can be formally summarized as follows:

*Problem 1:* Consider three UAV agents  $A_1, A_2, A_3$  moving with agent kinematics (1). Given pre-defined constant initial radial offset and radial increase rate coefficients  $a, b > 0$ , find an a monotonically increasing function  $\bar{\vartheta}(\cdot)$  satisfying  $\bar{\vartheta}(0) = 0$  and  $\lim_{t \rightarrow \infty} \bar{\vartheta}(t) = \infty$ , and generate the control signals  $\omega_i(t)$ ,  $\forall t \geq 0$  ( $i \in \{1, 2, 3\}$ ) such that

- (i)  $\|p_i(t) - p_j(t)\| - d_{ij}$ , where  $d_{ij} = 3$  km, is minimized for any  $i, j \in \{1, 2, 3\}$ ,  $i \neq j$  and any time  $t \geq 0$ .
- (ii) With  $p_c(t) \triangleq \frac{1}{3}(p_1(t) + p_2(t) + p_3(t))$  and  $r(t), \bar{\theta}(t)$  obeying (2),  $\|p_c(t) - (r(t) \cos \bar{\theta}(t), r(t) \sin \bar{\theta}(t))\|$  is minimized for any time  $t \geq 0$ .

Note that the requirements (i) and (ii) of Problem 1 imply the requirement of minimizing  $\|p_i(t) - (r(t) \cos \bar{\theta}(t), r(t) \sin \bar{\theta}(t))\| - d_{ic}$ , where  $d_{ic} = \sqrt{3}$  km ( $i \in \{1, 2, 3\}$ ).

#### D. Way-Point Assignment

Although Problem 1 describes the cooperative surveillance task formally, design of a control scheme directly based on this problem definition is not practical due to the time-indexed nature of the spiral path (2). For the purpose of refining Problem 1 and the path equation (2) in order to form a practical basis for control design, we define an ordered array of way-points over (2) in the form of

$$W = \left\{ w_n \right\}_{n=0}^{n=\bar{n}} \quad (3)$$

where the initial way-point is selected as the starting point of (2), i.e.  $w_0 = (a, 0)$ . The order of way-points obeys the time-ordering of their representation in (2), i.e. if for each  $0 \leq n \leq \bar{n}$  the polar coordinates of  $w_n$  are denoted by  $(r_{wn}, \bar{\theta}_{wn})$  and  $r_{wn} = a + b\bar{\nu}(t_n)$ , then  $t_n < t_{n+1}$  for any  $0 \leq n < \bar{n}$ . Furthermore, to assure the formation follows (2) within acceptable turning radius tolerances, it is arranged that the successive way-points satisfy  $\|w_n - w_{n+1}\| \leq 500$  m.

Based on the above assignment of way-points, Problem 1 can be refined for control design purposes as follows:

*Problem 2:* Consider three UAV agents  $A_1, A_2, A_3$  moving with agent kinematics (1). Given the way-points defined by (3), generate the control signals  $\omega_i(t)$ ,  $\forall t \geq 0$  ( $i \in \{1, 2, 3\}$ ) such that

- (i)  $\|p_i(t) - p_j(t)\| - d_{ij}$ , where  $d_{ij} = 3$  km, is minimized for any  $i, j \in \{1, 2, 3\}$ ,  $i \neq j$  and any time  $t \geq 0$ .
- (ii) For any time  $t \geq 0$  before reaching  $w_{\bar{n}}$ , with  $w_n$  being the last way-point visited (for some  $0 \leq n < \bar{n}$ ) at  $t$ ,  $\|p_c(t) - w_{n+1}\|$  is minimized.

### III. NON-HIERARCHICAL FORMATION CONTROL

In this section, we design a non-hierarchical decentralized control scheme for solving Problem 2. Before that, we present some background about *hierarchy*, *rigidity*, and *persistence*, which form a basis for the decentralized control scheme to be proposed.

#### A. Formation Control Structure and Hierarchy

In the formation control literature, two different types of formation control structures are used based on distribution of control tasks among agents; hierarchical and non-hierarchical. In a hierarchical structure, control tasks are classified and distributed non-uniformly among agents. A commonly used hierarchical structure within the formation control literature is the *leader-follower* structure [1], [9]. In the leader-follower structure, one “leader” agent is provided with direction and/or path information and is responsible for

path tracking, maneuvering and guiding tasks. The other “follower” agents within the formation measure their distances and/or bearings to a set of “leader” or “follower” agents or both, and are usually required to maintain the shape of the formation via keeping certain fixed distances. The tasks can be further prioritized among “follower” agents, e.g. there usually is a “first follower” agent that is responsible to keep a certain distance from the overall formation leader and at the same time perform a partial path tracking or formation orientation task.

For a non-hierarchical structure, the distance maintaining and path tracking tasks are uniformly distributed across the formation, i.e. the control tasks distributed to the agents are relatively identical. A typical non-hierarchical formation containing three agents is described in [10] under the name *three-coleader structure*. Our control design, to be presented in the sequel, is based on such a non-hierarchical structure.

Another type of classification of formation control structures for formation shape maintenance is in terms of the management of the distance keeping tasks between agent pairs. According to this classification a formation control structure is called *symmetric* if each inter-agent distance keeping task, say between agents  $A_i$  and  $A_j$  is performed via a simultaneous joint effort of both  $A_i$  and  $A_j$ , and called *asymmetric* if only one of the agents in each (or at least one) neighbor agent pair actively maintains the inter-agent distance for this pair, where a neighbor agent pair here denotes a pair of agents the distance between which is required to be maintained. According to this classification, the control structure we use for solving Problem 2 is an asymmetric one.

Note here that there are two key notions that are useful in formation shape maintenance studies and that form the basis for the classifications and the *three-coleader structure* mentioned above: *Rigidity* and *persistence*. In rough terms, a *rigid formation* is one in which the only smooth motions are those corresponding to translation or rotation of the whole formation, i.e. a smoothly moving *rigid formation* maintains its shape during motion once the nominated inter-agent distances are maintained. Again as a rough definition, a rigid formation with asymmetric control structure is further called *persistent* if it is possible to maintain the nominated inter-agent distances. Formal definitions and further details of *rigidity* and *persistence* can be found in [11], [12] and the references therein.

#### B. Decentralized Control Design

Given the background above, we design a non-hierarchical decentralized formation control scheme for Problem 2. The main motivation behind using a non-hierarchical control structure as opposed to a hierarchical one is the assumption that the non-hierarchical structure has a more balanced distribution of the formation maintenance and path tracking tasks among the individual agents. Hence it is expected to be more robust to speed variations among the agents and atmospheric disturbances.

For each agent  $A_i$  ( $i \in \{1, 2, 3\}$ ) we design an individual controller inputs of which at each time instant  $t \geq 0$  are positions  $p_i(t)$ ,  $p_j(t)$ ,  $w_{n+1}$  of, respectively, itself, the agent  $A_j$  it follows, and the next way-point to visit (as described in Problem 2). We shall first state the law, which is rather complicated, and then motivate it. The overall form of the law involves determining a *desired heading* for an agent, and changing its actual heading towards the desired heading; the determination of the desired heading can be complicated, and may involve a *desired position*. The individual controller output is the angular velocity  $\omega_i(t)$  in (1). A proportional-integral (PI) feedback control law, with proportional gain  $k_p > 0$  and integral gain  $k_i > 0$ , is proposed to generate  $\omega_i$ :

$$\omega_i(t) = k_p[\theta_{id}(t) - \theta_i(t)] + k_i \int_{t_0}^t [\theta_{id}(t) - \theta_i(t)] dt \quad (4)$$

where  $\theta_i(t)$  and  $\theta_{id}(t)$  are, respectively, the actual and desired headings of agent  $A_i$ . The *desired heading signal*  $\theta_{id}(t)$  is generated according to requirements of Problem 2, using the following switching law:

$$\theta_{id}(t) = \begin{cases} \bar{\theta}_{id}(t) & \text{if } d_{min} < \|w_{n+1} - p_j(t)\| < d_{max} \\ \theta_{ic}(t) + \pi & \text{else if } \|w_{n+1} - p_i(t)\| \leq d_{ic} \\ \theta_{ic}(t) & \text{else} \end{cases} \quad (5)$$

$$\bar{\theta}_{id}(t) = \begin{cases} \theta_{id1}(t) & \text{if } |e_{ij}| > \varepsilon_i \text{ or } |e_{ic}| > \varepsilon_i \\ \theta_{id2}(t) & \text{else} \end{cases} \quad (6)$$

where  $d_{min} \triangleq d_{ij} - d_{ic}$ ,  $d_{max} \triangleq d_{ij} + d_{ic}$ ,  $e_{ij} \triangleq \|p_i(t) - p_j(t)\| - d_{ij}$ ,  $e_{ic} \triangleq \|p_i(t) - w_{n+1}\| - d_{ic}$ ,  $\theta_{id1}(t) \triangleq \angle(\bar{p}_{id}(t) - p_i(t))$ ,  $\theta_{id2}(t) \triangleq \angle(\bar{p}_{id}(t) - \bar{p}_{id}(t - T_\Delta))$ ,  $\theta_{ic}(t) \triangleq \angle(w_{n+1} - p_i(t))$ ;  $d_{ij}$ ,  $d_{ic}$  are as defined in Section II,  $T_\Delta > 0$  is a certain delay term used for interpolation, and  $\varepsilon_i$  is a separation tolerance term.  $\bar{p}_{id}(t)$  is the refined form of the *desired position term*  $p_{id}(t)$ , which is defined, for the case  $C(p(t), d_{ic}) \cap C(p_j(t), d_{ij}) \neq \emptyset$ , by the circle intersection rule

$$p_{id} = \arg \min \{ \|p - p_i\| \mid p \in C(w_{n+1}, d_{ic}) \cap C(p_j, d_{ij}) \} \quad (7)$$

where  $C(p, r)$  ( $p \in \mathbb{R}^2, r \in \mathbb{R}^+$ ) denotes the circle with center  $p$  and radius  $r$ , similarly to [12], [13]. The refined form of  $p_{id}$  is given by

$$\bar{p}_{id} = \begin{cases} p_{id} & \text{if } C(p, d_{ic}) \cap C(p_j, d_{ij}) \neq \emptyset \\ w_{n+1} + \frac{e_{jiw} + d_{ic} \operatorname{sgn}(e_{jiw})}{2\|p_j - w_{n+1}\|} (p_j - w_{n+1}) & \text{else} \end{cases} \quad (8)$$

where  $e_{jiw} \triangleq \|p_j - w_{n+1}\| - d_{ij}$ . The second line of (8) gives the point which has minimal equidistance from  $C(w_{n+1}, d_{ic})$  and  $C(p_j(t), d_{ij})$ , in case these two circles do not intersect. Note that it is desired to have  $p_{id}$  defined all the time; the refined desired position  $\bar{p}_{id}$  is introduced only to well-define the terms  $\theta_{id2}(t)$  in the switching law (6), for the cases where  $C(w_{n+1}, d_{ic})$  and  $C(p_j(t - T_\Delta), d_{ij})$  do not intersect as well as the cases they intersect.

Note here that for the ideal case with no major disturbances,  $C(w_{n+1}, d_{ic}) \cap C(p_j(t), d_{ij})$  is expected to be non-empty. However, significant disturbance sources (speed

differences between the individual agents as well as sensor and actuator noises) may cause the circles  $C(w_{n+1}, d_{ic})$  and  $C(p_j(t), d_{ij})$  to non-intersect. In such a case the control law (4) together with the first two lines of the switching law (5) is designed to move agent  $A_j$  in a way to force these two circles to intersect again.

The reasoning behind different heading cases of the switching law (5) is as follows (each case number corresponding to the line order in (5)):

Case 1a:  $C(w_{n+1}, d_{ic}) \cap C(p_i(t), d_{ij})$  is non-empty and  $|e_{ij}|$  or  $|e_{ic}|$  is larger than the tolerance bound  $\varepsilon_i$ , the agent  $A_i$  is not close enough to any intersection point of the circles  $C(w_{n+1}, d_{ic})$  and  $C(p_j(t), d_{ij})$ . Therefore,  $A_i$  is forced to head towards the closest intersection point of the two circles, and the agent heading becomes  $\theta_{id1}(t) = \angle(\bar{p}_{id}(t) - p_i(t))$

Case 1b:  $C(w_{n+1}, d_{ic}) \cap C(p_i(t), d_{ij})$  is non-empty and both  $|e_{ij}|$  and  $|e_{ic}|$  are smaller than the tolerance bound  $\varepsilon_i$ , the agent  $A_i$  is sufficiently close to the desired location  $\bar{p}_{id}(t)$  in (8). In this case, in order to avoid slowing of the motion,  $A_i$  is headed towards an interpolated target point based on the current and past value of  $\bar{p}_{id}$ , using the agent heading  $\theta_{id2}(t) = \angle(\bar{p}_{id}(t) - \bar{p}_{id}(t - T_\Delta))$ .

Case 2:  $C(w_{n+1}, d_{ic}) \cap C(p_i(t), d_{ij})$  is empty due to the fact that  $p_i(t)$  is too close to  $w_{n+1}$ . Therefore, denoting the agent that follows  $A_i$  by  $A_k$ ,  $p_{kd} = \arg \min \{ \|p - p_k\| \mid p \in C(w_{n+1}, d_{ic}) \cap C(p_i, d_{ik}) \}$  is undefined, which is an undesired situation for  $A_k$ . In order to make the intersection non-empty, the agent  $A_i$  is forced to head away from  $w_{n+1}$  in the direction  $\theta_{ic}(t) = \angle(p_i(t) - w_{n+1})$

Case 3:  $C(w_{n+1}, d_{ic}) \cap C(p_j(t), d_{ij})$  is empty because the separation distance between  $p_j(t)$  and  $w_n$  is too large. This leads to the undesired situation for the following agent  $A_k$  described in Case 1. In order to make the intersection non-empty, the agent  $A_i$  is forced to head towards  $w_{n+1}$  in the direction  $\theta_{ic}(t) = \angle(w_{n+1} - p_i(t))$

In our design and simulation studies, the values of the delay and tolerance terms are taken as  $T_\Delta = 1$  sec and  $\varepsilon_i = 30$  m.

In the next section, we numerically analyze the decentralised control scheme with the individual agent control law (4),(5) using a series of simulations with various settings.

#### IV. SIMULATION-BASED ANALYSIS

In all of the simulations presented in this section, the parameters of the spiral surveillance trajectory (2) are taken as  $a = 0$  and  $b = \frac{6000}{2\pi}$  and, as mentioned in Section III, the desired separation distances are set to  $d_{12} = d_{23} = d_{31} = 3$  km and  $d_{ic} = \sqrt{3}$  km ( $i \in \{1, 2, 3\}$ ), and the region  $R_S$  to be surveyed is a 30 km  $\times$  30 km square. The decentralised control laws (4)–(5) are applied using design parameters  $k_P = 2$ ,  $k_I = 0.0005$  and switching tolerance  $\varepsilon_i = 30$  m.

In the following three subsections, we present the simulation results and discussions for three different cases<sup>1</sup>. In addition to Remark 1, note that all the parameter values used in the simulations and the analysis are practical ones based on specifications supplied by the DSTO.

#### A. The Case with Equal Agent Speeds and No Disturbance

As the first case, we assume that all agents fly with the same constant speed of 32 m/s and there exists no noise affecting the system. The results are shown in Figure 2, which demonstrates that both the path tracking and formation maintenance tasks are successfully achieved within acceptable distant tolerances.

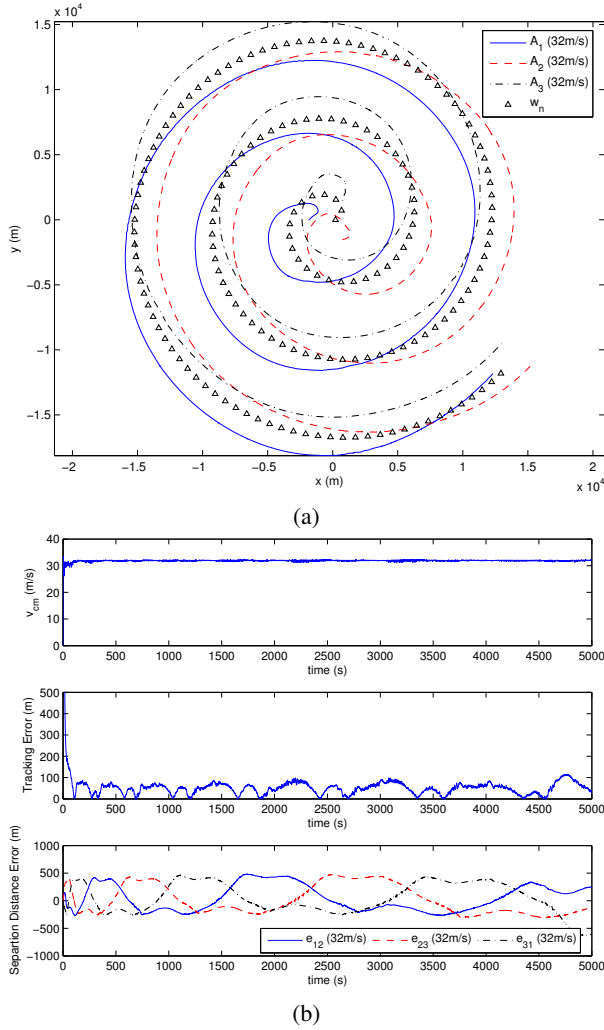


Fig. 2. Surveillance simulation with  $v_{c1} = v_{c2} = v_{c3} = 32$  m/s: (a) Motion trajectories of the individual agents. (b) Speed  $v_{cm}$  of the CM of the formation, distance of CM to the path to be tracked, and inter-agent distance-keeping errors  $e_{12}$ ,  $e_{23}$ ,  $e_{31}$  during surveillance.

#### B. Effects of Speed Variations

As the second case, we consider agents flying at different constant speeds close to the maximal value of 32 m/s and

<sup>1</sup>Space limitations prevent the reporting of the cases with noisy measurements and sensor actuator errors, which is however treated in an extended version of this paper that can be obtained from the authors in preprint form.

assume that there exists no noise affecting the system.

The control laws (4)–(5) are applied to various simulation settings with different UAV speeds, where  $A_1$  is always assigned a constant speed of 32 m/sec and each of  $A_2$  and  $A_3$  is assigned a constant speed between 28 m/s–32 m/s. Figure 3 shows the simulation results for a sample case with  $v_{c1} = 32$  m/s,  $v_{c2} = 30.5$  m/s,  $v_{c3} = 28$  m/s. Figure

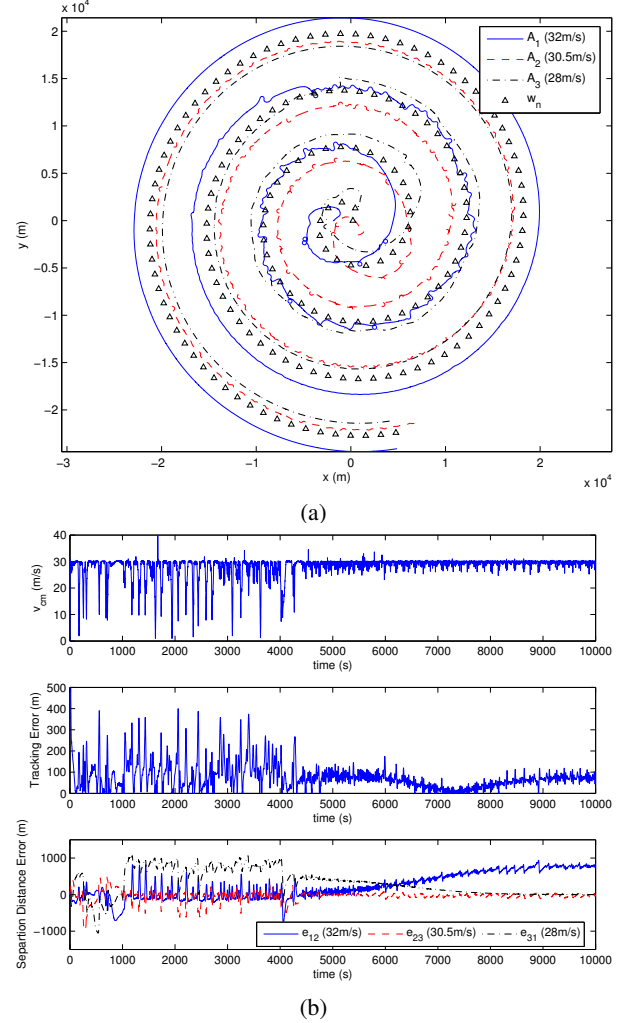


Fig. 3. Surveillance simulation with  $v_{c1} = 32$  m/s,  $v_{c2} = 30.5$  m/s,  $v_{c3} = 28$  m/s: (a) Motion trajectories of the individual agents. (b) Speed  $v_{cm}$  of the CM of the formation, distance of CM to the path to be tracked, and inter-agent distance-keeping errors  $e_{12}$ ,  $e_{23}$ ,  $e_{31}$  during surveillance.

3 demonstrates that even under speed variations between the individual agents the separation distances  $d_{12}$ ,  $d_{23}$  and  $d_{31}$  are maintained within allowable tolerances and the maximum errors of  $e_{12}$ ,  $e_{23}$ ,  $e_{31}$  don't exceed 1 km, 1/3 of the required inter-agent distance.

The results of a series of simulations with various different agent speed combinations is summarized in Figure 4. Figure 4(a) shows the root mean square distance  $\bar{e}_{cm}$  of the formation CM position  $p_c(t)$  to the spiral path (2) versus a set of agent speeds  $v_{c2}$  and  $v_{c3}$  over a time span  $t_f$ :

$$\bar{e}_{cm} = \sqrt{\frac{1}{t_f} \int_0^{t_f} (p_c(t) - r(t))^2 dt} \quad (9)$$

Figure 4(b) shows the mean difference  $e_{v_{cm}} = v_{ave} - \frac{1}{t_f} \int_0^{t_f} v_{cm}(t) dt$  between the average speed  $v_{ave} = (v_{c1} + v_{c2} + v_{c3})/3$  of the three agents and the speed  $v_{cm}(t) = \|\dot{p}_c(t)\|$  of the CM of the formation versus agent speeds  $v_{c2}$  and  $v_{c3}$ .

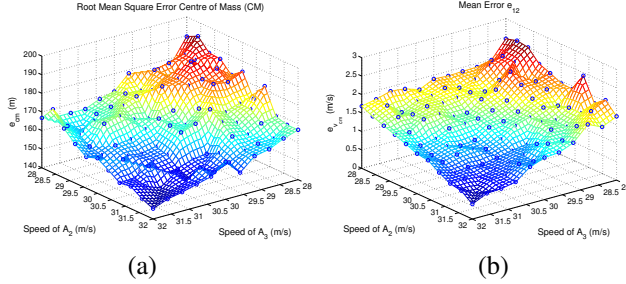


Fig. 4. (a) Root-mean-square of the distance between the actual and desired locations of the formations CM versus  $v_{c2}$  and  $v_{c3}$ . (b) Error between the actual speed of CM and average speed of all agents.

### C. Effects of Wind Disturbance

As the last simulation case, we consider an external wind disturbance affecting all the three agents, which are assumed to fly with the same speed of 32 m/s. We model the wind disturbance on each agent  $A_i$  ( $i \in \{1, 2, 3\}$ ) as a disturbance velocity vector  $\eta_i(t) = (\dot{x}_{wi}(t), \dot{y}_{wi}(t))$ , affecting  $(\dot{x}_i(t), \dot{y}_i(t))$  in (1) additively, where  $\dot{x}_{wi}(t) = B_{wi} \cos(\alpha_{wi})$ ,  $\dot{y}_{wi}(t) = B_{wi} \sin(\alpha_{wi})$ . Here, the magnitude  $B_{wi}(t)$  is assumed to have a Gaussian random value at each time  $t$ , with mean  $\mu_w$  and variance  $\sigma_w^2$ . Note here that the values of  $\mu_w$  and  $\sigma_w^2$  are the same for all three agents but the random value of  $B_{wi}(t)$  are generated separately and may be different for different values of the  $t, i$  pair.  $\alpha_{wi}$  is assumed to be constant and selected as  $\alpha_{wi} = \frac{\pi}{4}$  rad in our simulations.

A set of simulations is conducted with  $\mu_w$  taking values within 0–10 (m/s) and  $\sigma_w$  within 0–4 (m/s). The simulation results have demonstrated that wind disturbances with mean  $\mu_w \leq 4$  m/s and standard deviation  $\sigma_w^2 \leq 4$  m/s do not have very significant influence on the formation's path tracking and inter-agent distance keeping performance. Above these limits, it is observed that the formation slows down as a whole ( $v_{cm} < v_{ave}$ ) but the inter-agent distance keeping errors stay within acceptable tolerances.

## V. CONCLUDING REMARKS

In this paper we have considered the problem of formation controlling a team of three UAVs, where the UAVs have to maintain an equilateral triangular formation, with the CM following a nominated surveillance trajectory. For this particular problem we have proposed a decentralized non-hierarchical formation scheme involving proportional-integral control with certain switching terms. We have demonstrated via simulations that the above problem is successfully solved by the proposed control scheme for the case where all the UAV speeds are equal and there is no external (wind) disturbance.

Later we have examined the affects of differences between individual UAV speeds and wind disturbances via an extensive number of simulation tests. The simulation results

demonstrate that the formation maintenance and trajectory tracking tasks are met within feasible separation and tracking error limits, even when the UAV speeds are different, provided that the speed differences are smaller than a certain bound. The allowed speed difference tolerance is found to be sufficiently large. For the case of differences between the individual UAV speeds we have found prove by conducting a series of simulations with different individual UAV speeds up to a certain speed difference between the UAVs, that the formation is maintained.

The robustness properties of the proposed control scheme with respect to wind disturbances are found to be similar to those with respect to UAV speed differences. That is such disturbance sources are allowable, with resulting separation and tracking errors within feasible limits, within certain magnitude bounds with significant values.

Potential future research topics include formal mathematical analysis of the stability and robustness properties of the proposed scheme, revision of the control laws for making them more robust to internal and external disturbances and UAV speed differences, and enhancing the path tracking and formation maintenance performances.

## REFERENCES

- [1] A. K. Das, R. Fierro, V. Kumar, J. P. Ostrowski, J. Spletzer, and C. J. Taylor, "A vision-based formation control framework," *IEEE Trans. on Robotics and Aut.*, vol. 18, no. 5, pp. 813–825, October 2002.
- [2] M. Polycarpou, Y. Yang, Y. Liu, and K. Passino, *Cooperative Control: Models, Applications and Algorithms*. Kluwer Academic, 2003, ch. Coop. Control Design for Uninhabited Air Vehicles, pp. 283–321.
- [3] I.-A. F. Ihle, J. Jouffroy, and T. I. Fossen, "Formation control of marine surface craft: A lagrangian approach," *IEEE Journal of Oceanic Engineering*, vol. 31, no. 4, pp. 922–934, October 2006.
- [4] A. W. Stroupe, M. C. Martin, and T. Balch, "Distributed sensor fusion for object position estimation by multi-robot systems," *Proc. IEEE Int. Conf. on Robotics and Aut.*, vol. 2, pp. 1092–1098, May 2001.
- [5] J. R. Spletzer and C. J. Taylor, "Dynamic sensor planning and control for optimally tracking targets," *The International Journal of Robotics Research*, vol. 22, no. 1, pp. 7–20, 2003.
- [6] A. N. Bishop, B. Fidan, B. D. O. Anderson, K. Dogancay, and P. N. Pathirana, "Optimality analysis of sensor-target geometries in passive localization: Part 1 - bearing-only localization," in *Proc. 3rd Int. Conf. on Intelligent Sensors, Sensor Networks and Information Processing (ISSNIP)*, Melbourne, VIC, Australia, December 2007, pp. 7–12.
- [7] S. Drake, K. Brown, J. Fazackerley, and A. Finn, "Autonomous control of multiple UAVs for the passive location of radars," *Proc. Int. Conf. on Intelligent Sensors, Sensor Networks and Information Processing (ISSNIP)*, pp. 403–409, December 2005.
- [8] D. Ledger, "Electronic warfare capabilities of mini UAVs," in *Prod. the Electronic Warfare Conference.*, Kuala Lumpur, 2002.
- [9] H. G. Tanner, G. J. Pappas, and V. Kumar, "Leader-to-formation stability," *IEEE Trans. on Robotics and Automation*, vol. 20, no. 3, pp. 443–455, June 2004.
- [10] B. D. O. Anderson, C. Yu, S. Dasgupta, and A. S. Morse, "Control of a three coleaders formation in the plane," *Systems and Control Letters*, vol. 56, pp. 573–578, 2007.
- [11] J. M. Hendrickx, B. D. O. Anderson, J.-C. Delvenne, and V. D. Blondel, "Directed graphs for the analysis of rigidity and persistence in autonomous agent systems," *International Journal of Robust and Nonlinear Control*, vol. 17, pp. 960–981, July 2007.
- [12] B. Fidan, B. D. O. Anderson, C. Yu, and J. M. Hendrickx, *Modeling and Control of Complex Systems*. Taylor&Francis, 2007, ch. Persistent Autonomous Formations and Cohesive Motion Control, pp. 247–275.
- [13] S. Sandeep, B. Fidan, and C. Yu, "Decentralized cohesive motion control of multi-agent formations," in *Proc. 14th Mediterranean Conference on Control and Automation*, June 2006, pp. 1–6.